Journal of Experimental Botany, Vol. 70, No. 18 pp. 4807–4818, 2019
doi:10.1093/jxb/erz208 Advance Access Publication May 6, 2019
This paper is available online free of all access charges (see https://academic.oup.com/jxb/pages/openaccess for further details)

RESEARCH PAPER

Elevated CO_2-induced changes in mesophyll conductance and anatomical traits in wild type and carbohydrate-metabolism mutants of Arabidopsis

Yusuke Mizokami[1,2,*], Daisuke Sugiura[3,*], Chihiro K. A. Watanabe[2], Eriko Betsuyaku[4], Noriko Inada[5] and Ichiro Terashima[2]

[1] Commissariat à l'Energie Atomique et aux Energies Alternatives, Centre National de la Recherche Scientifique, UMR 7265 Biologie Végétale et Microbiologie Environnementale, Aix Marseille Université, Saint-Paul-lez-Durance, France
[2] Department of Biological Sciences, Graduate School of Science, The University of Tokyo, Bunkyo, Tokyo 113-0033, Japan
[3] Graduate School of Bioagricultural Sciences, Nagoya University, Chikusa, Nagoya 464-8601, Japan
[4] Faculty of Life and Environmental Sciences, University of Tsukuba, Tsukuba, Ibaraki 305-8577, Japan
[5] Graduate School of Life and Environmental Sciences, Osaka Prefecture University, Sakai, Osaka 599-8531, Japan

*Correspondence: yusuke.mizokami@gmail.com or daisuke.sugiura@gmail.com

Received 30 December 2018; Editorial decision 24 April 2019; Accepted 25 April 2019

Editor: Tracy Lawson, University of Essex, UK

Abstract

Decreases in photosynthetic rate, stomatal conductance (g_s), and mesophyll conductance (g_m) are often observed under elevated CO_2 conditions. However, which anatomical and/or physiological factors contribute to the decrease in g_m is not fully understood. *Arabidopsis thaliana* wild-type and carbon-metabolism mutants (*gwd1*, *pgm1*, and *cfbp1*) with different accumulation patterns of non-structural carbohydrates were grown at ambient (400 ppm) and elevated (800 ppm) CO_2. Anatomical and physiological traits of leaves were measured to investigate factors causing the changes in g_m and in the mesophyll resistance (expressed as the reciprocal of mesophyll conductance per unit chloroplast surface area facing to intercellular space, S_c/g_m). When grown at elevated CO_2, all the lines showed increases in cell wall mass, cell wall thickness, and starch content, but not in leaf thickness. g_m measured at 800 ppm CO_2 was significantly lower than at 400 ppm CO_2 in all the lines. Changes in S_c/g_m were associated with thicker cell walls rather than with excess starch content. The results indicate that the changes in g_m and S_c/g_m that occur in response to elevated CO_2 are independent of non-structural carbohydrates, and the cell wall represents a greater limitation factor for g_m than starch.

Keywords: *Arabidopsis thaliana*, cell wall thickness, elevated CO_2, mesophyll conductance, mesophyll resistance, non-structural carbohydrates, Rubisco.

Introduction

Mesophyll conductance (g_m) describes the diffusivity of CO_2 from the intercellular space to the site of CO_2 fixation in the chloroplast stroma as it passes through the cell wall, cell membrane, cytosol, and the chloroplast envelope. Three major methods have been used to estimate g_m; A–C_i curve-fitting (Ethier and Livingston, 2004), chlorophyll fluorescence (Harley *et al.*, 1992), and carbon isotope discrimination (Evans *et al.*, 1986). The magnitude of the resulting value of g_m expressed on

a leaf-area basis is comparable to that of the stomatal conductance (g_s), the measure of CO_2 diffusion from the ambient air to the intercellular space (e.g. Tazoe *et al.*, 2011; von Caemmerer and Evans 2015). Thus, g_m represents a significant limitation to photosynthesis. Both g_s and g_m are known to change considerably depending on environmental conditions and plant growth status (Farquhar and Sharkey, 1982; von Caemmerer and Evans, 2015). Determining how the factors underlying g_m respond to environmental conditions and their differences between species will increase our understanding of plant biomass production.

Among the components that influence g_m, the cumulative surface area of the chloroplasts positioned along the cell membrane facing the intercellular space (S_c) and the cell wall thickness are the most crucial anatomical factors. Tholen *et al.* (2008) demonstrated that g_m increases with an increase in S_c in photoreceptor mutants of Arabidopsis that showed marked differences in chloroplast positioning. Adachi *et al.* (2013) also found close relationships between S_c, g_m, and maximum photosynthetic rate in inbred lines of *Oryza sativa*. In C_3 plants, it is estimated that cell wall resistance accounts for 50% of the mesophyll resistance, the inverse of g_m (Evans *et al.*, 1994, 2009; Terashima *et al.*, 2011). Scafaro *et al.* (2011) found that two wild *Oryza* relatives that had thicker cell walls than *O. sativa* showed greater drawdown of CO_2 from the intercellular space to the chloroplast stroma. It has also been argued that extreme enlargement of starch grains would distort the chloroplasts (Cave *et al.*, 1981; Delucia *et al.*, 1985; Pritchard *et al.*, 1997), causing suppression of photosynthesis by the hindrance of CO_2 diffusion in the liquid phase (Nafziger and Koller, 1976; Nakano *et al.*, 2000; Sawada *et al.*, 2001).

Some species show decreases in g_m in response to instantaneous increases in ambient CO_2 concentration in the short-term (Flexas *et al.*, 2007a; Tazoe *et al.*, 2011); however, in other species including soybean and wheat g_m remains virtually unchanged (Bernacchi *et al.*, 2005; Tazoe *et al.*, 2009). We have previously examined responses to elevated CO_2 in Arabidopsis wild-type and stomatal-function mutants, and found that g_s and g_m respond independently to changes in CO_2 concentration(Mizokami *et al.*, 2019). The mechanisms associated with the decrease in g_m in response to CO_2 differ from those in response to water deficit, in which ABA plays a key role (Mizokami *et al.*, 2015).

There are some reports that growth at elevated CO_2 results in a decrease in g_m in some species. It has been debated whether such interspecific differences in g_m responses to the growth CO_2 concentration can be explained by changes in cell wall thickness and/or starch content. For example, Zhu *et al.* (2012) reported that under free-air CO_2 enrichment conditions, cell wall thickness significantly increased in rice but not in wheat, and a decrease in g_m was found only in rice. Kitao *et al.* (2015) found a negative correlation between g_m and starch content in the leaves of *Betula platyphylla* (Japanese white birch) grown under ambient or elevated CO_2. Thus, an increase in cell wall thickness and/or starch accumulation may cause a decrease in g_m at elevated CO_2. However, the contribution of each of these factors to the increase in resistance to CO_2 diffusion has not yet been fully elucidated since they usually occur simultaneously.

Teng *et al.* (2006) found that growth of Arabidopsis at elevated CO_2 resulted in cell wall thickening, although the effects on S_c, g_m, and photosynthesis were not reported. Given this fact, it should be possible to separately evaluate the effects of wall thickness and non-structural carbohydrates on g_m by using Arabidopsis carbohydrate-metabolism mutants grown at ambient or elevated CO_2. In this study, selected the Col-0 wild-type and three mutants of that are deficient in α-glucan/water dikinase (GWD1), plastidic phosphoglucomutase (PGM1), and cytosolic fructose 1, 6-bisphosphatase (CFBP1), which are key enzymes in starch breakdown, starch synthesis, and sucrose synthesis, respectively. Leaves of *gwd1* show excess starch accumulation (Zeeman *et al.*, 2004), leaves of *pgm1* are starchless but show relatively high sugar concentrations (Periappuram *et al.*, 2000), and leaves of *cfbp1* are expected to show reduced sucrose content. The photosynthetic capacity of *gwd1* is comparable to that of Col-0, whereas that of *pgm1* and *cfbp1* are significantly lower, especially when plants are grown at elevated CO_2 (C.K.A. Watanabe *et al.*, unpublished results). In addition to these mutants, we grew wild-type plants for an extended period with either low or high nitrogen availability at either ambient or elevated CO_2 in order to obtain a wide range of control data. We also considered the reciprocal of mesophyll conductance per unit chloroplast surface area, i.e. mesophyll resistance per unit chloroplast surface area (S_c/g_m), which might be directly related to the resistance associated with cell wall thickness (Evans *et al.*, 2009). Sugars and starch tend to accumulate at elevated CO_2, which may cause the down-regulation of photosynthesis due to a decrease in Rubisco content and activity (Sheen, 1994; Krapp and Stitt, 1995). We paid particular attention to the down-regulation of photosynthesis due to accumulation of non-structural carbohydrates.

Materials and methods

Plant material and growth conditions

We used *Arabidopsis thaliana* (L.) Heynh. accessions Col-0 (wild-type,WT), and the mutants CS3093 (At1g10760; *gwd1/sex1*), CS210 (At5g51820; *pgm1*), and SALK_064456C (At1g43670; *cfbp1/fins1*). *cfbp1* corresponds to *fins1* (Cho and Yoo, 2011). These mutants are each deficient in one of the enzymes related to carbohydrate metabolism, as follows: chloroplastic glucan water dikinase 1 (*gwd1*), chloroplastic phosphoglucomutase 1 (*pgm1*), and cytosolic fructose-1, 6-bisphosphatase 1 (*cfbp1*).

Seeds of all the accessions were sown in a mixture of autoclaved Metro Mix 350 (Sun Gro Horticulture, Bellevue, WA, USA) and vermiculite (1:1, v/v) in 200-ml plastic pots. The pots were placed in a cold room at 4 °C for two nights and transferred to two CO_2-controlled growth chambers (LPH-0.5P-SH, Nippon Medical & Chemical Instruments).

Plants were grown at a photosynthetically active photon flux density (PFD) of 200 μmol m^{-2} s^{-1} provided by fluorescent lamps during an 8-h light period, with day/night temperatures of 23/21 °C, and a relative humidity of 60%. The CO_2 concentrations in the growth chambers were controlled at either 400 ppm (ambient, aCO_2) or 800 ppm (elevated, eCO_2).

For the first week, plants were irrigated with deionized water. From the second week, they were irrigated with modified Hoagland solution 2–3 times a week. The solution contained 1.5 mM $MgSO_4$, 1.35 mM NaH_2PO_4, 0.1 mM NaCl, 0.05 mM Fe-EDTA, 0.05 mM H_3BO_3, 0.01 mM $MnSO_4$, 0.001 mM $ZnSO_4$, 1 μM $CuSO_4$, 0.5 μM Na_2MoO_4,

0. 2 μM $CoSO_4$. High- and low-nitrogen solutions of 8 mM N and 1 mM N, respectively, with 5 mM K^+ and 5 mM Ca^{2+} were obtained by adding KNO_3, $Ca(NO_3)_2$, KCl, and $CaCl_2$.

WT plants irrigated with the high-nitrogen solution and grown for a total of 39–42 d are hereafter referred to as Col_{HN}, whilst WT plants irrigated with the low-nitrogen solution and grown for 38–42 d are referred to as Col_{LN}. To obtain leaves with different photosynthetic traits, some Col_{HN} plants were grown for a further 2 weeks (a total of 50–52 d) and these are referred to as Col_{50}. The *gwd1*, *pgm1*, and *cfbp1* plants were irrigated with the high-nitrogen solution. Col_{HN}, Col_{LN}, and *cfbp1* were grown for 38–42 d after sowing, whilst *gwd1* and *pgm1* were grown for 50–52 d after sowing due to their slower growth rates. Measurements of photosynthesis and the various traits were conducted on young mature leaves, which were the 11th–14th leaves to emerge.

Gas exchange and isotope measurements

Photosynthesis measurements were conducted during the second half of the light period. Gas exchange measurements were performed using a laboratory-made leaf cuvette (50×55×20 mm) designed for a single leaf of Arabidopsis (Tholen *et al.*, 2008; Mizokami *et al.*, 2015, 2019). All gas exchange measurements to evaluate photosynthetic traits were conducted at 1% O_2 to minimize the effect of photorespiration on g_m, using cylinders containing 100% N_2, 100% O_2, and 1% CO_2, which were mixed using mass-flow controllers (MM-3102L-NN, LINTEC, Tokyo, Japan). The O_2 concentration of the gas was checked using an oxygen sensor (3080-O_2, Walz, Effeltrich, Germany).

Light was provided by a metal halide lamp (PCS-UMX250, NPI, Tokyo, Japan). The PFD at the leaf level was monitored using a GaAs photodiode (G1738, Hamamatsu Photonics, Hamamatsu, Japan) placed in the chamber during the measurements. The GaAs sensor was calibrated against a quantum sensor (LI-190SA, LI-COR, Lincoln, NE, USA). The concentrations of CO_2 and H_2O in the air entering and leaving the cuvette were monitored using an infrared gas analyser (LI-7000, Li-Cor). The O_2 effect on the sensitivity of the infrared CO_2/H_2O analyser was corrected following Mizokami *et al.* (2015).

To measure photosynthesis at different levels of CO_2, we placed two leaves from two different plants together in the leaf cuvette. The leaf temperature and vapor pressure deficit (VPD) were kept at 22.5 °C and 0.85 kPa, respectively, and PFD was set to 1000 μmol photons m^{-2} s^{-1}. For the plants grown at aCO_2, the first measurement was taken at an ambient CO_2 concentration (C_a) of 400 ppm, and then C_a was switched to 800 ppm. For the plants grown at eCO_2, the first measurement was taken at 800 ppm, and then C_a was switched to 400 ppm. Gas exchange parameters were recorded when the photosynthesis attained a steady-state rate, and the photosynthetic rates and stomatal conductance measured at C_a of 400 ppm (A_{400} and g_{s400}) and 800 ppm (A_{800} and g_{s800}) were obtained. The air entering and leaving the cuvette was collected in 30-ml Pyrex bottles with two stopcocks, and the $^{13}C/^{12}C$ ratios were measured with a mass spectrometer (IsoPrime 100, IsoPrime Ltd, Manchester, UK) to obtain mesophyll conductance at the two C_a levels (g_{m400} and g_{m800}).

Calculation of mesophyll conductance

Mesophyll conductance was calculated as described by Tazoe *et al.* (2011):

$$g_m = \frac{\left(b - a_i - \frac{eR_d}{A+R_d}\right)\frac{A}{C_a}}{a_b + (a_s - a_b)\frac{C_s}{C_a} + (b - a_s)\frac{C_i}{C_a} - \frac{eR_d(C_i - \Gamma^*)}{C_a(A+R_d)} - \frac{f\Gamma^*}{C_a} - \Delta}$$

where C_a is the ambient CO_2 concentration, C_s is the CO_2 at the leaf surface, C_i is the intercellular CO_2, C_c is the CO_2 in the chloroplast stroma, a_b and a_s are the carbon isotope discriminations caused by diffusion through the boundary layer (2.9‰) and stomata (4.4‰), respectively, a_i is the carbon isotope discrimination during CO_2 diffusion/dissolution through water (1.8‰), b is the carbon isotope discrimination caused by the carboxylation reaction by Rubisco and phosphoenolpyruvate carboxylase (30‰), e is the discrimination in respiration (calculated as described by Tazoe *et al.*, 2009, 2011), and Δ is the measured carbon isotope discrimination (Evans *et al.*, 1986). The factor e required a correction because $\delta^{13}C$ during plant growth was different to that during measurement (Wingate *et al.*, 2007), its values were set to –24.4‰ and –17.5‰ for plants grown at aCO_2 and eCO_2, respectively, as described by Mizokami *et al.* (2019). f is the carbon isotope discrimination during photorespiration (11.6‰) and $\Gamma^\star$ is the CO_2 compensation point without day respiration (Lanigan *et al.*, 2008). R_d is the day respiration rate. For $\Gamma^\star$ and R_d at 1% O_2, we assumed values for Arabidopsis Col-0 grown at aCO_2 and eCO_2 previously estimated by (Mizokami *et al.*, 2019) using the Laisk method (Laisk, 1977). For the plants grown at aCO_2, $\Gamma^\star$ and R_d were 11.3 μmol mol^{-1} and 0.53 μmol m^{-2} s^{-1}, respectively, whilst for the plants grown at eCO_2, $\Gamma^\star$ and R_d were 5.4 μmol mol^{-1} and 0.45 μmol m^{-2} s^{-1}, respectively. Although the values of $\Gamma^\star$ at 1% O_2 were higher than those estimated by Walker and Cousins (2013) in a previous study, a sensitivity analysis has shown that variations in $\Gamma^\star$ have a minor impact on g_m (Mizokami *et al.*, 2019). We did not apply the ternary correction (Farquhar and Cernusak, 2012) since the VPD (0.872±0.083 kPa) and transpiration rate (0.0018±0.0005 mol m^{-2} s^{-1}) were sufficiently low in our present study: for Col-0 grown at aCO_2 we determined that g_{m400} calculated with or without the ternary correction differed by only 0.005 mol m^{-2} s^{-1}, and g_{m800} differed by only 0.0031 mol m^{-2} s^{-1}.

Sampling

The leaves from the two plants that had been used for the photosynthesis measurements were subsequently sampled for microscopic and biochemical analyses. Two or three similarly aged leaves including leaves used for the photosynthesis measurements were sampled to determine leaf morphological traits, leaf nitrogen content, $\delta^{13}C$, and the content of non-structural carbohydrates (starch and soluble sugars). Discs were taken from the leaves and measurements were taken after drying. The other two or three similarly aged leaves were stored at –80 °C for later determination of Rubisco content and cell wall content. In total, 4–6 leaves were sampled from the two plants and the set of data obtained from them was dealt with as one biological replicate.

Light and transmission electron microscope analyses

Small lamina segments were cut with a razor blade, immediately immersed in 0.2 M sodium cacodylate buffer (pH 7.0) containing 2.5% paraformaldehyde and 2% glutaraldehyde, and vacuum-infiltrated until most of the segments sank. They were then stored at 4 °C overnight. The segments were post-fixed in 1% OsO_4 for 1 h and dehydrated in an ethanol series. Some segments were embedded in Technovit 7100 (Heraus Holding, Hanau, Germany) and used for light-microscope analysis. The other segments were further dehydrated in a series of propylene oxide and embedded in Spurr's resin for TEM analysis.

For light microscopy, leaf transverse sections of 1 μm thick were cut on an ultramicrotome (Reichert Ultracut S, Leica, Vienna, Austria) with a glass knife and stained with a 0.1% (w/v) Toluidine Blue solution in 1% (w/v) sodium borate. Leaf thickness, the surface area of mesophyll cell walls exposed to the intercellular space (S_{mes}, m^2 m^{-2}), and the surface area of chloroplasts facing the intercellular space (S_c, m^2 m^{-2}) were determined for each replicate. S_{mes} and S_c were calculated using the curvature correction factor following Thain (1983) and Evans *et al.* (1994). The mean value of the correction factor was 1.24 in the present study. For TEM, ultrathin sections of 70 nm thick were cut on the ultramicrotome with a diamond knife (Ultra 45°, Diatome AG, Switzerland) and placed on a 150-mesh copper grid. The grids were stained with a 2% uranyl acetate solution followed by a lead citrate solution. The sections were examined on a JEM-1010 TEM (JEOL, Japan). The wall thickness of mesophyll cells was measured on the ultrathin sections using the ImageJ software (Schneider *et al.*, 2012). The thickness was calculated for randomly selected cells by dividing the cross-sectional area of the cell wall by its length. On average, 58 μm of cell wall length was analysed for each plant.

Leaf mass per unit area and non-structural carbohydrates

The 2–3 dried leaf discs were weighed to determine leaf mass per area (LMA, g m^{-2}) and then ground with a Multi-beads Shocker (Yasui Kikai,

Osaka, Japan). The ground samples (3–5 mg each) were then used to determine the contents of glucose, sucrose, and starch according to Araya *et al.* (2006). Soluble sugars were extracted with 80% ethanol, and sucrose was hydrolysed to glucose and fructose with an invertase solution (Wako Chemical, Osaka, Japan). The precipitate was treated with amyloglucosidase (A-9228, Sigma-Aldrich, St. Louis, MO) to break down starch into glucose. Finally, glucose, and glucose equivalents of sucrose and starch, were quantified using a Glucose CII test kit (Wako Chemicals). The content of sugars and starch were expressed on a leaf-area basis. Structural LMA (sLMA, g m^{-2}) consisting of proteins, minerals, lipids, and soluble and insoluble phenolics (Poorter *et al.*, 2006) was calculated by subtracting the content of non-structural carbohydrates from LMA (Bertin *et al.*, 1999).

Nitrogen and $\delta^{13}C$

The nitrogen content (Nmass, g N g^{-1}) and $\delta^{13}C$ of the ground leaf samples were determined with a CN analyser (Vario Micro, Elementar Analyzensysteme GmbH, Hanau, Germany) connected to an isotopic ratio mass spectrometer (IsoPrime100, IsoPrime, Manchester, UK). N content per area (N_{area}, g N m^{-2}) was calculated as a product of Nmass and LMA. $\delta^{13}C$ (‰) as follows:

$$\delta^{13}C = \frac{R_{sample} - R_{standard}}{R_{standard}} \times 1000$$

where R_{sample} and $R_{standard}$ are the $^{13}C/^{12}C$ ratios of the sample and the standard (PDB, 0.011180).

Rubisco and cell wall contents

The two or three frozen leaf discs were used to determine the contents of Rubisco and cell wall materials as described previously (Mizokami *et al.*, 2015; Sugiura *et al.*, 2017). The frozen discs were homogenized in Tris–HCl buffer (62.5 mM, pH 6.8) using a Multi-beads Shocker (Yasui Kikai) to extract Rubisco. After extraction, SDS–PAGE, Coomassie Brilliant Blue staining, and formamide (NACALAI TESQUE, Kyoto, Japan) extraction were conducted and the Rubisco content was determined by measuring absorbance of the extract at 595 nm. From the residual pellet after the Rubisco extraction, starch was removed using amyloglucosidase and the cytoplasmic protein was removed using 1 M NaCl, and the resultant pellet was assumed to contain the cell wall materials. The pellet was weighed after drying, and cell wall mass per area (CMA, g m^{-2}) was calculated.

$\Delta(S_c/g_{m400})$, Δcell wall thickness, and Δstarch

Because g_m is proportional to the surface area available for diffusion, it is sometimes expressed as per unit chloroplast surface area adjacent to the intercellular airspaces (g_m/S_c; Terashima *et al.*, 2011). Because it is the resistance that is expected to be linearly related to cell wall thickness, we used the reciprocal of the conductance per S_c in our analyses, i.e. S_c/g_{m400}. S_c/g_{m400} and the draw-down of CO_2 from the intercellular space to the site of carboxylation in the chloroplast (C_i–C_c) were then related to cell wall thickness and starch content. To quantify the effect of growth CO_2 on S_c/g_{m400}, we used ΔX (%), the percent change in the trait X between the plants grown at eCO_2 and those grown at aCO_2 normalized to those grown at aCO_2, as follows:

$$X = \frac{X_{eCO_2} - X_{aCO_2}}{X_{aCO_2}} \times 100$$

ΔX was calculated for S_c/g_{m400}, cell wall thickness, and starch content.

Statistical analysis

Statistical tests were performed using Systat13 (Systat Software, Richmond, CA, USA). The effects of growth CO_2 on anatomical, morphological, physiological, and photosynthetic traits were evaluated by ANOVA followed by Tukey's multiple comparison test. $\delta^{13}C$ of the leaves was compared only by Tukey's test at each growth CO_2 level since $\delta^{13}C$ in the air differed depending on the growth chambers. Photosynthetic traits were also compared between the CO_2 concentrations during the measurements by Student's *t*-test.

Results

Leaf anatomical traits

Leaf anatomical traits of the different Arabidopsis lines were analysed using light and electron micrographs of leaf transverse sections (Supplementary Figs S1, S2 at *JXB* online) and were found to differ markedly (Table 1). Only the cell wall thickness was increased significantly by growth at eCO_2. The thickness was greatest in Col_{50} and lowest in *cfbp1* at both aCO_2 and eCO_2 (Table 1, Supplementary Fig. S2). Thickness was greater in eCO_2 by ~20–35% in the WT and *pgm1*, whereas it did not differ in *gwd1* or *cfbp1*. Leaf thickness, S_c, S_m, and S_c/S_m were greatest in *pgm1*, but the differences between the mutants and the WT were small.

Leaf morphological and physiological traits

Leaf morphological and physiological traits were determined for the leaves that had been used for the photosynthesis measurements. LMA, sLMA, and CMA were greater in the eCO_2 samples, and they differed significantly among the lines (Fig. 1). In both aCO_2 and eCO_2 plants LMA was highest in *gwd1* whilst sLMA and CMA were highest in *pgm1*. These traits tended to be greater in Col_{50} than Col_{HN}.

The level of non-structural carbohydrates was also increased by elevated growth CO_2. The starch content was highest in *gwd1* (the starch-excess mutant) and lowest in *pgm1* (Fig. 2A). Within the WT, the starch content was highest in Col_{LN} in both aCO_2 and eCO_2. Soluble sugars were highest in *pgm1*, followed by *gwd1* (Fig. 2B). Chloroplasts with excess starch were clearly visible in light and electron micrographs of *gwd1*, whilst starchless chloroplasts could be seen in *pgm1* (Supplementary Figs S1, S2).

N_{area} was slightly increased by elevated growth CO_2, whereas Rubisco content was not (Table 1). N_{area} was highest in *pgm1* and lowest in Col_{LN} in both aCO_2 and eCO_2. The Rubisco content in Col_{LN} grown at eCO_2 was significantly lower than in the other lines, but otherwise no other differences were observed. There was a positive correlation between the Rubisco content and N_{area} among the WT and mutants *gwd1* and *cfbp1* grown at aCO_2 and eCO_2 (Supplementary Fig. S3). However, *pgm1* did not fit this pattern, having relatively low Rubisco content despite having the highest N_{area}.

$\delta^{13}C$ differed significantly among the lines (Table 1), with the highest value in *gwd1* and lowest in *pgm1* in both aCO_2 and eCO_2. The WT showed intermediate values for both aCO_2 and eCO_2. There were negative relationships between $\delta^{13}C$ and C_c (Supplementary Fig. S4A, B) and positive correlations between $\delta^{13}C$ value and starch content for all the lines (Supplementary Fig. S4C, D).

Table 1. *Anatomical and physiological traits of Arabidopsis Col-0 and carbohydrate-mutants grown under ambient CO_2 (aCO_2, 400 ppm) or elevated CO_2 (eCO_2, 800 ppm)*

	Growth CO_2	Col_{HN}	Col_{50}	Col_{LN}	*gwd1*	*pgm1*	*cfbp1*
Leaf thickness (μm)	aCO_2 (ns)	201.8±28.3b	216.6±32.7b	221.6±13.8b	223.6±20.7b	306.0±39.6a	184.4±6.0b
	eCO_2	202.4±24.0B	191.9±19.5B	215.5±23.0B	233.1±17.4B	355.2±69.4A	193.2±25.0B
Cell wall thickness (μm)	aCO_2**	0.233±0.023ab	0.286±0.032a	0.221±0.032ab	0.247±0.012ab	0.246±0.012ab	0.210±0.059b
	eCO_2	0.317±0.033A	0.336±0.063A	0.257±0.024AB	0.246±0.052AB	0.295±0.059AB	0.195±0.015B
S_c (m^2 m^{-2})	aCO_2 (ns)	6.52b±0.49b	8.29±1.26b	7.59±0.52b	7.76±1.52b	12.82±1.22b	6.54±1.12b
	eCO_2	7.15±1.21B	8.19±0.80B	8.22±0.85B	7.88±2.09B	14.63±3.21A	6.78±0.34B
S_m (m^2 m^{-2})	aCO_2 (ns)	8.41±0.58b	10.13±1.72b	9.53±0.91b	10.19±1.47b	14.15±1.63a	8.37±1.54b
	eCO_2	9.19±1.43B	10.29±1.00B	9.98±1.34B	9.90±2.24B	16.17±3.57A	8.31±0.30B
S_c/S_m (m^2 m^{-2})	aCO_2 (ns)	0.776±0.054b	0.820±0.038ab	0.798±0.022b	0.757±0.057b	0.908±0.032a	0.784±0.056b
	eCO_2	0.777±0.017B	0.797±0.044B	0.828±0.065AB	0.790±0.050B	0.904±0.031A	0.816±0.033AB
N_{area} (g N m^{-2})	aCO_2**	1.167±0.078c	1.391±0.060b	0.881±0.139d	1.194±0.039c	1.731±0.085a	1.071±0.070c
	eCO_2	1.227±0.066BC	1.427±0.133B	0.813±0.123D	1.342±0.049B	1.979±0.110A	1.120±0.033C
Rubisco (g m^{-2})	aCO_2**	1.050±0.278a	1.061±0.111a	0.852±0.112a	1.015±0.045a	1.183±0.076a	1.175±0.148a
	eCO_2	1.271±0.078A	1.091±0.148A	0.695±0.110B	1.128±0.044A	1.151±0.093A	1.158±0.149A
$\delta^{13}C$ (‰)	aCO_2	–32.5±0.34b	–33.0±0.19ab	–32.5±0.29bc	–32.0±0.19c	–33.5±0.14a	–32.6±0.23b
	eCO_2	–40.4±0.48AB	–39.3±0.24C	–39.6±0.10BC	–38.9±0.28C	–41.2±0.56A	–40.9±0.65A

S_c is the chloroplast surface area exposed to the intercellular space; S_m is the mesophyll surface area exposed to the intercellular space; and N_{area} is leaf nitrogen content per area. Values are means (±SD), n=4. The overall effect of growth CO_2 was evaluated by ANOVA (**P<0.01; ns, P>0.05), except for $\delta^{13}C$ (see Methods). Significant differences within each CO_2 treatment were determined using ANOVA followed by Tukey's test (P<0.05), and are indicated by different letters (lower-case for aCO_2, upper-case for eCO_2).

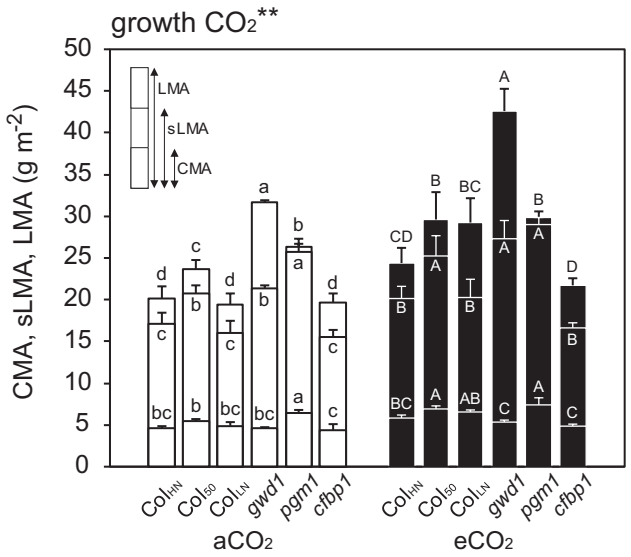

Fig. 1. Leaf mass per area (LMA), structural leaf mass per area (sLMA), and cell wall mass per area (CMA) in leaves of Arabidopsis Col-0 grown with high nitrogen for 39–42 d (Col_{HN}), with low nitrogen for 38–42 d (Col_{LN}), or with high nitrogen for 50–52 d (Col_{50}), and the carbohydrate-metabolism mutants *gwd1*, *pgm1*, and *cfbp1* grown under either ambient CO_2 (aCO_2, 400 ppm) or elevated CO_2 (eCO_2, 800 ppm). Data are means (±SD), n=4. The overall effect of growth CO_2 was evaluated by ANOVA and is indicated above the graph (**P<0.01). Significant differences among the lines within each CO_2 treatment were determined using ANOVA followed by Tukey's test (P<0.05), and are indicated by different letters (lower-case for aCO_2, upper-case for eCO_2).

Leaf photosynthetic characteristics

Photosynthesis measurements were conducted at 400 ppm CO_2 (A_{400}, g_{s400}, and g_{m400}) and 800 ppm (A_{800}, g_{s800}, and g_{m800}) for plants grown at aCO_2 and eCO_2.

A_{400} and A_{800} were higher in the WT and *gwd1* than in *pgm1* and *cfbp1* at both aCO_2 and eCO_2 (Fig. 3A, B). A_{800} was significantly lower than A_{400} in Col_{HN}, Col_{50}, and Col_{LN} at aCO_2 (Fig. 3A), and also significantly lower in Col_{HN}, Col_{50}, *pgm1*, and *cfbp1* at eCO_2 (Fig. 3B). g_{s400} and g_{s800} were lowest in *pgm1* at both aCO_2 and eCO_2 (Fig. 3C, D). g_{s800} was significantly lower than g_{s400} in all the lines at both aCO_2 and eCO_2. g_{m400} and g_{m800} were lowest in *cfbp1* at both aCO_2 and eCO_2 (Fig. 3E, F). g_{m800} was significantly lower than g_{m400} in all the lines at both aCO_2 and eCO_2 (Fig. 3C, D) except for *cfbp1* at aCO_2 and *pgm1* at eCO_2. Although the photosynthetic rates (A_{400} and A_{800}) and mesophyll conductances (g_{m400} and g_{m800}) were not significantly affected by growth CO_2 conditions, g_{m400} was slightly lower in the WT and *pgm1* grown at eCO_2. Stomatal conductance (g_{s400} and g_{s800}) was significantly increased by elevated growth CO_2, especially in *gwd1*, *pgm1*, and *cfbp1*.

Factors that determine photosynthetic characteristics

Relationships among photosynthetic characteristics and various morphological and physiological traits were analysed to determine which traits were involved in the responses to growth CO_2 conditions. Here, we focus on the photosynthetic characteristics measured at 400 ppm CO_2.

There was a positive correlation between A_{400} and Rubisco content for the WT and *gwd1*, whereas *pgm1* and *cfbp1* showed lower photosynthetic rates despite having high Rubisco contents (Fig. 4A). The relationship between A_{400} and g_{s400} was not significant (Fig. 4B); however, A_{400} was positively correlated with g_{m400} for all the lines except for *pgm1* (Fig. 4C).

Relationships among photosynthetic characteristics and accumulation of sugars and starch were investigated to determine whether feedback regulation was occurring (Fig. 5). No negative correlations with the soluble sugar or starch contents were

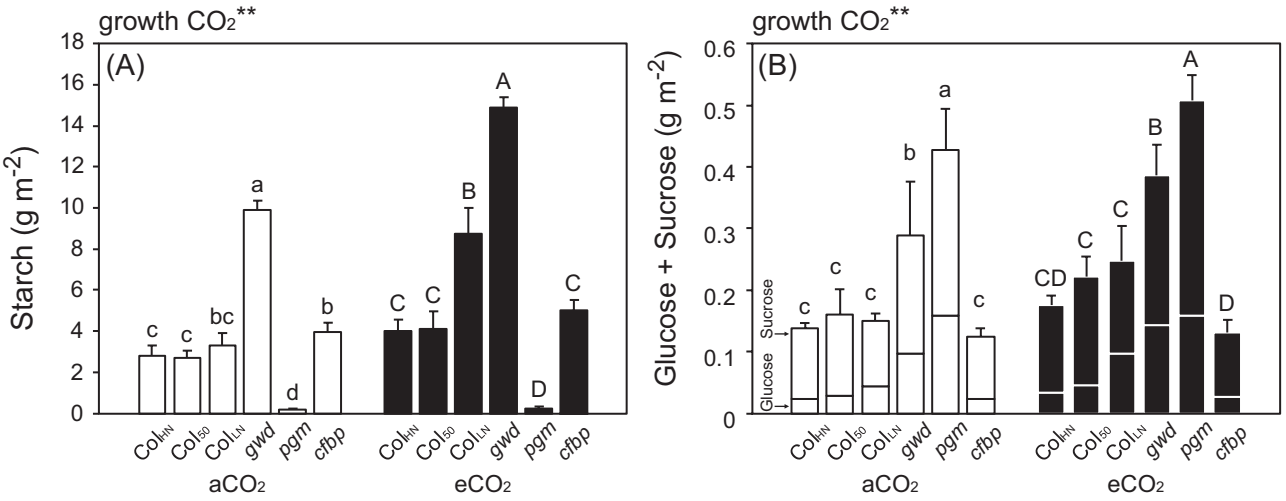

Fig. 2. (A) Starch and (B) soluble sugars in the leaves of Arabidopsis Col-0 grown with high nitrogen for 39–42 d (Col_{HN}), with low nitrogen for 38–42 d (Col_{LN}), or with high nitrogen for 50–52 d (Col_{50}), and the carbohydrate-metabolism mutants *gwd1*, *pgm1*, and *cfbp1* grown under ambient CO_2 (aCO_2, 400 ppm) or elevated CO_2 (eCO_2, 800 ppm). Data are means (±SD), n=4. The overall effect of growth CO_2 was evaluated by ANOVA and is indicated above the graph (**P<0.01). Significant differences among the lines within each CO_2 treatment were determined using ANOVA followed by Tukey's test (P<0.05), and are indicated by different letters (lower-case for aCO_2, upper-case for eCO_2).

found for either Rubisco content (Fig. 5A, B), A_{400} (Fig. 5C, D), or g_{m400} (Fig. 5E, F).

Relationships between the mesophyll conductance and morphological and anatomical features were investigated. There was no overall relationship between S_c/g_{m400} and cell wall thickness among the lines (Fig. 6A); however, within each line S_c/g_{m400} increased with the increase in cell wall thickness. No relationship was observed between S_c/g_{m400} and starch content among the lines (Fig. 6B). The draw-down of CO_2 from the intercellular space to the site of carboxylation in the chloroplast (C_i–C_c) was positively correlated with cell wall thickness for all the lines except for *pgm1* (Fig. 6C). There was no clear relationship between C_i–C_c and starch content among the lines (Fig. 6D). Cell wall thickness was positively correlated with cell wall mass per area (CMA) for all the lines and CMA was also positively correlated with sLMA (Supplementary Fig. S5B, C). We also expected a positive correlation between mesophyll conductance and S_c, but no clear relationship was found (Supplementary Fig. S6).

We examined how the changes in the cell wall thickness and starch content in response to growth CO_2 conditions affected mesophyll resistance using $\Delta S_c/g_{m400}$, the percentage change in a given line between the plants grown at eCO_2 and those grown at aCO_2 normalised to aCO_2. $\Delta S_c/g_{m400}$ showed a strong positive correlation with ΔCell wall thickness but there was no clear correlation between $\Delta S_c/g_{m400}$ and ΔStarch content (Fig. 7A, B).

Discussion

The cell wall is a greater limiting factor for g_m than starch content

Our results indicated that among the changes in various morphological, anatomical, and physiological traits that we observed, the increases in cell wall mass and thickness in Arabidopsis had the major impact on mesophyll conductance. The excess accumulation of starch was not linked to a decrease in g_m (Fig. 5F), whereas within each line the increase in cell wall thickness was associated with an increase in mesophyll resistance, S_c/g_m (Fig. 6A), and a greater draw-down of CO_2 from the intercellular space to the chloroplast, C_i–C_c (Fig. 6C). It was clear that the percentage change in mesophyll resistance between eCO_2 and aCO_2 plants ($\Delta S_c/g_{m400}$) was associated with the percentage change in cell wall thickness (ΔCell wall thickness) across all lines (Fig. 7A). The fact that there was no clear correlation between $\Delta S_c/g_{m400}$ and ΔStarch indicated the lack of effect of the latter (Fig. 7B). The measurement of cell wall thickness requires observations with an electron microscope and is therefore laborious, whereas measurement of cell wall mass is relatively easy. Since cell wall thickness was highly correlated with cell wall mass per area (CMA, Supplementary Fig. S5A), the latter could be an alternative indicator of cell wall thickness when investigating the environmental responses of g_m in the same species. As also shown in a previous study (Sugiura *et al.*, 2017), there was a strong positive correlation between CMA and sLMA (Supplementary Fig. S5B), indicating that sLMA could also be an efficient parameter within a plant species that reflects the thickness and mass of the cell wall.

When plants are grown under elevated CO_2 conditions, increases are observed in the thickness and mass of cell walls (Teng *et al.*, 2006) and in the accumulation of non-structural carbohydrates (Kitao *et al.*, 2015; Sugiura *et al.*, 2017), whilst decreases are observed in g_m (Zhu *et al.*, 2012). It has been proposed that excess accumulation of starch in mesophyll cells could hinder CO_2 diffusion and result in decreased g_m (Nafziger and Koller, 1976; Nakano *et al.*, 2000; Sawada *et al.*, 2001). Zhu *et al.* (2012) reported a decrease in g_m and an increase in starch content in flag-leaves of rice grown with free-air CO_2 enrichment); however, inter-relationships among the traits were not examined in detail. In our present study, although the starch-excess mutant *gwd1* accumulated starch at

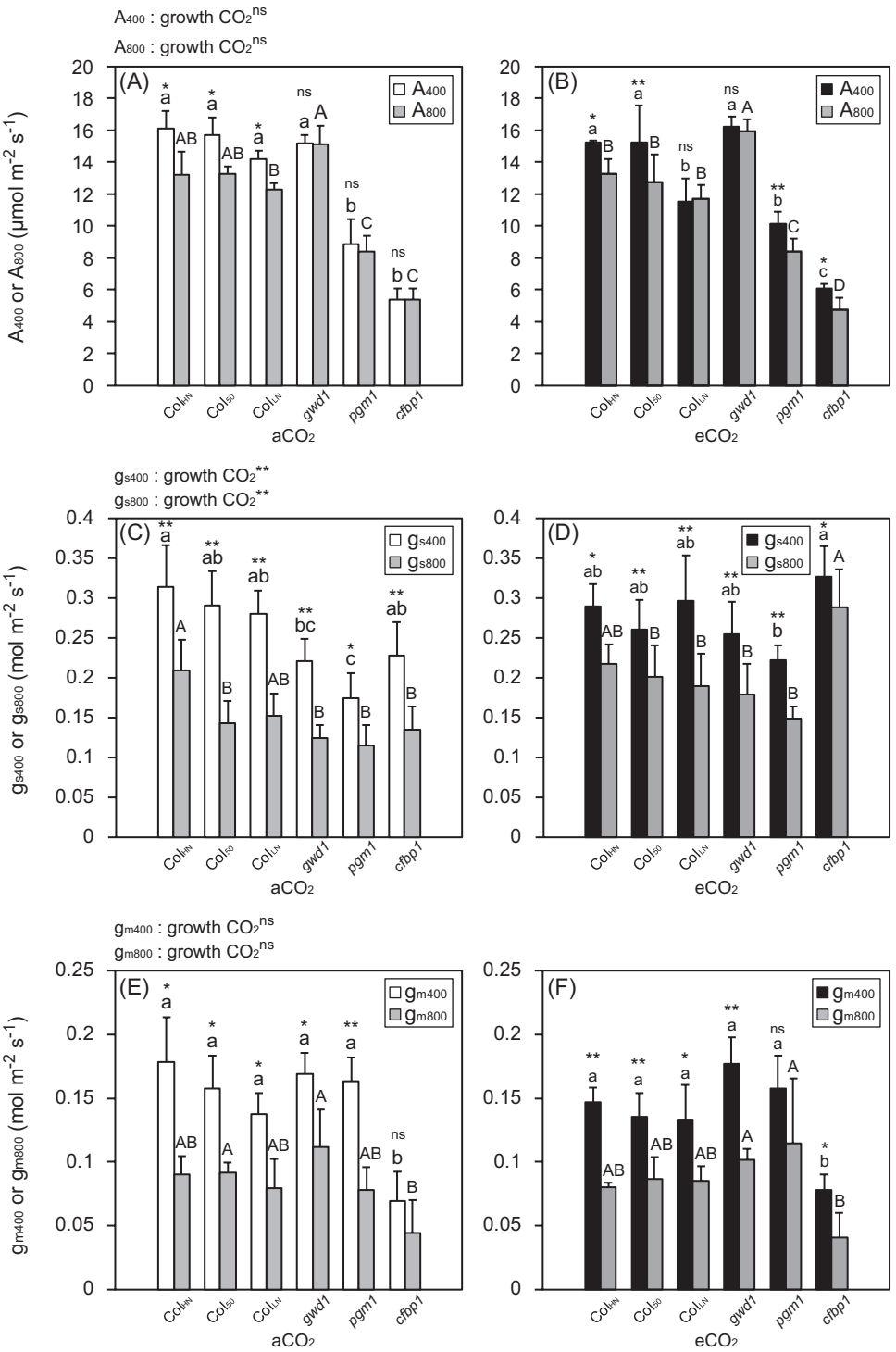

Fig. 3. Photosynthetic characteristics of Arabidopsis Col-0 grown with high nitrogen for 39–42 d (Col_{HN}), with low nitrogen for 38–42 d (Col_{LN}), or with high nitrogen for 50–52 d (Col_{50}), and the carbohydrate-metabolism mutants *gwd1*, *pgm1*, and *cfbp1* grown under ambient CO_2 (aCO_2, 400 ppm) or elevated CO_2 (eCO_2, 800 ppm). (A, B) Photosynthetic rates measured at 400 ppm CO_2 (A_{400}) and 800 ppm CO_2 (A_{800}) for plants grown in (A) aCO_2 and (B) eCO_2. (C, D) Stomatal conductance measured at 400 ppm CO_2 (g_{s400}) and 800 ppm CO_2 (g_{s800}) for plants grown in (A) aCO_2 and (B) eCO_2. (E, F) Mesophyll conductance measured at 400 ppm CO_2 (g_{m400}) and 800 ppm CO_2 (g_{m800}) for plants grown in (A) aCO_2 and (B) eCO_2. Data are means (±SD), n=4. The overall effect of growth CO_2 was evaluated by ANOVA (**P<0.01; ns, P>0.05). Significant differences among the lines within each growth CO_2 treatment were determined using ANOVA followed by Tukey's test (P<0.05), and are indicated by different letters (lower-case for aCO_2, upper-case for eCO_2). Significant differences between measurements at 400 ppm CO_2 and 800 ppm CO_2 within each line were determined using Student's t-test (**P<0.01; *P<0.05; ns, P>0.05).

both aCO_2 and eCO_2 (Fig. 2A), g_m did not decrease (Fig. 3E, F). Our results suggested that direct effects of non-structural carbohydrates on CO_2 diffusion and g_m were minor, whereas the increased cell wall mass and thickness caused a decrease in g_m and an increase in S_c/g_m under elevated CO_2 conditions (Table 1, Figs 1, 7A). Thus, we conclude that the increases in

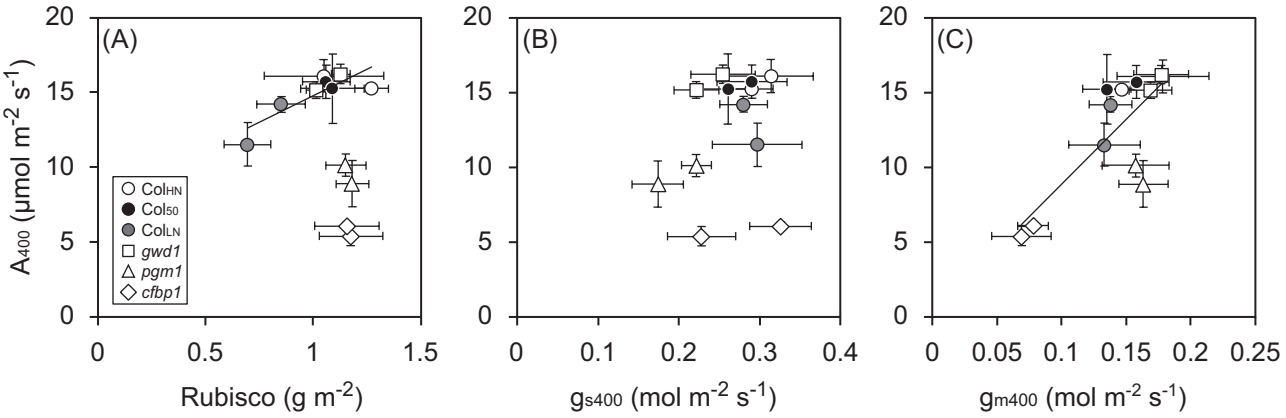

Fig. 4. Relationships between photosynthetic rate, Rubisco content per area, stomatal conductance, and mesophyll conductance measured at 400 ppm CO_2 for Arabidopsis lines grown under ambient CO_2 (aCO_2, 400 ppm) or elevated CO_2 (eCO_2, 800 ppm). The lines, as indicated in the key in (A), were Col-0 grown with high nitrogen for 39–42 d (Col_{HN}), with low nitrogen for 38–42 d (Col_{LN}), or with high nitrogen for 50–52 d (Col_{50}), and the carbohydrate-metabolism mutants *gwd1*, *pgm1*, and *cfbp1*. (A) Photosynthetic rate (A_{400}) and Rubisco content per area, (B) A_{400} and stomatal conductance (g_{s400}), and (C) A_{400} and mesophyll conductance (g_{m400}). Data are means (±SD), n=4. Regression lines are shown in (A) for Col_{HN}, Col_{50}, Col_{LN}, and *gwd1* (R^2=0.68), and in (C) for Col_{HN}, Col_{50}, Col_{LN}, *gwd1*, and *cfbp1* (R^2=0.60).

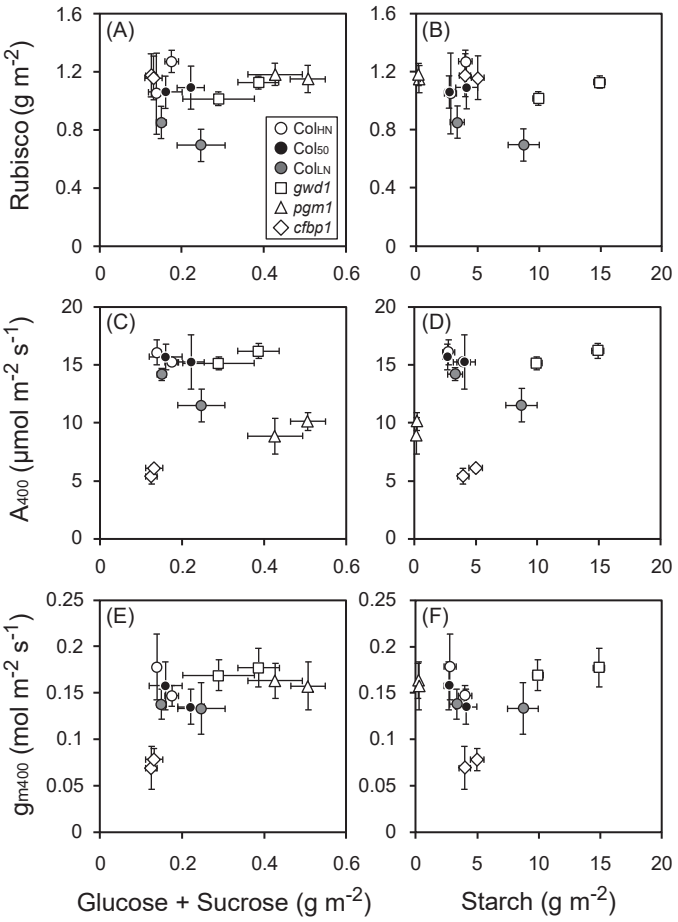

Fig. 5. Relationships between photosynthetic characteristics measured at 400 ppm CO_2 and content of soluble sugars (glucose and sucrose) and starch for Arabidopsis lines grown under ambient CO_2 (400 ppm) or elevated CO_2 (800 ppm). The lines, as indicated in the key in (A), were Col-0 grown with high nitrogen for 39–42 d (Col_{HN}), with low nitrogen for 38–42 d (Col_{LN}), or with high nitrogen for 50–52 d (Col_{50}), and the carbohydrate-metabolism mutants *gwd1*, *pgm1*, and *cfbp1*. Rubisco versus contents of glucose and sucrose (A) and versus starch (B), photosynthetic rate (A_{400}) versus contents of glucose and sucrose (C) and versus starch (D), and mesophyll conductance (g_{m400}) versus contents of glucose and sucrose (E) and versus starch (F). Data are means (±SD), n=4.

cell wall mass and thickness contributed more to the decrease in g_m and the increase in S_c/g_m than starch has been observed to do in previous studies.

Although we found a simultaneous increase in S_c/g_m and cell wall thickness in each individual line, there was not a positive correlation between them overall across all lines (Fig. 6A). The fact that Col_{LN}, *pgm1*, and *cfbp1* showed different patterns suggests that variation in other physiological processes and anatomical features could also be involved. Mesophyll conductance can be separated into gaseous and liquid phases, and the liquid phase can be further separated into five phases, namely cell wall, plasma membrane, cytosol, chloroplast envelope, and stroma (Evans *et al.*, 2009). It is considered that CO_2 diffusion across the cell wall and across the plasma membrane are the major limiting steps (Terashima *et al.*, 2011). In recent years, it has been suggested that aquaporins—proteins involved in water transport in the plasma membrane—may affect the permeability of CO_2 through membranes (Terashima *et al.*, 2006; Mori *et al.*, 2014; Groszmann *et al.*, 2017). Therefore, it is possible that Col_{LN} grown under low N availability showed higher S_c/g_{m400} regardless of the thinner cell wall due to a lower expression of aquaporins in the plasma membranes. The expression levels of aquaporins are significantly decreased in roots of *Oryza sativa* grown under low N availability (Ishikawa-Sakurai *et al.*, 2014), so it is possible that a similar effect may occur in the leaf mesophyll cells in Arabidopsis. In *cfbp1*, in which the sucrose synthesis pathway is impaired, the photosynthetic rate, A_{400}, was limited by the low g_m (Figs 3, 4A) even though this line showed a high value of N_{area}, high Rubisco content, and the thinnest cell walls (Table 1). Therefore, factors other than cell wall thickness, such as the plasma membrane, cytoplasm, chloroplast envelope, might be markedly changed in *cfbp1*. Furthermore, since the composition of the cell wall is markedly different among carbohydrate-metabolism mutants of Arabidopsis, including *pgm1* and *gwd1* (Engelsdorf *et al.*, 2017), it is possible that differences in the porosity of the cell wall affected g_m in these mutants, as discussed by Evans *et al.* (2009). Future

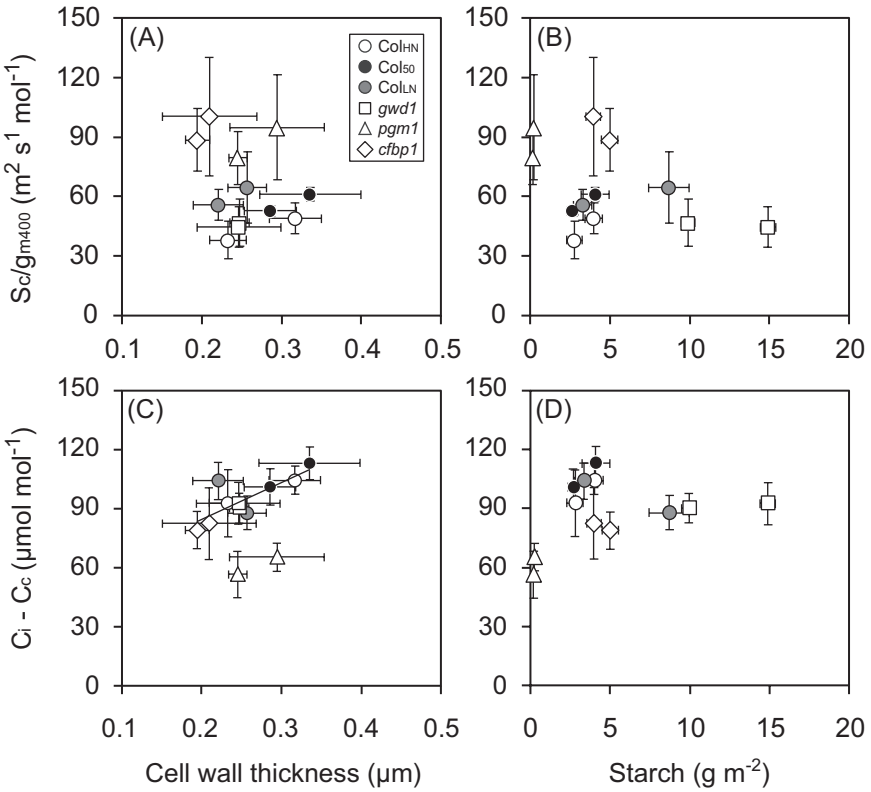

Fig. 6. Relationships between mesophyll resistance and draw-down of CO_2 from intercellular space to the chloroplast (C_i–C_c) measured at 400 ppm CO_2 and cell wall thickness and starch content for Arabidopsis lines grown under ambient CO_2 (400 ppm) or elevated CO_2 (800 ppm). The lines, as indicated in the key in (A), were Col-0 grown with high nitrogen for 39–42 d (Col_{HN}), with low nitrogen for 38–42 d (Col_{LN}), or with high nitrogen for 50–52 d (Col_{50}), and the carbohydrate-metabolism mutants *gwd1*, *pgm1*, and *cfbp1*. Mesophyll resistance (S_c/g_{m400}) versus cell wall thickness (A) and versus starch content (B), and draw-down of CO_2 versus cell wall thickness (C) and versus starch content (D). Data are means (±SD), n=4. The regression line for Col_{HN}, Col_{50}, Col_{LN}, *gwd1*, and *cfbp1* is shown in (C) (R^2=0.65).

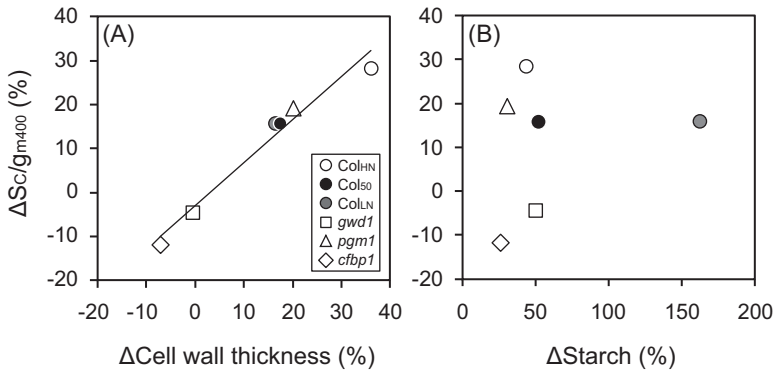

Fig. 7. Relationships between changes in mesophyll resistance and changes in cell wall thickness and starch content in response to CO_2 growth conditions for Arabidopsis lines grown under ambient CO_2 (400 ppm) or elevated CO_2 (800 ppm). The lines, as indicated in the key in (A), were Col-0 grown with high nitrogen for 39–42 d (Col_{HN}), with low nitrogen for 38–42 d (Col_{LN}), or with high nitrogen for 50–52 d (Col_{50}), and the carbohydrate-metabolism mutants *gwd1*, *pgm1*, and *cfbp1*. Percentage change in mesophyll resistance ($\Delta S_c/g_{m400}$) measured at 400 ppm CO_2 versus (A) percentage change in cell wall thickness (ΔCell wall thickness) and versus percentage change in starch content (ΔStarch). For calculation of the percentage changes see Methods. Data are means (±SD), n=4. The regression line for all the data is shown in (A) (R^2=0.97).

metabolomic, transcriptomic, and micro-anatomical studies will be required to elucidate the mechanisms underlying the changes in g_m in these mutants.

It is reported that g_m in plants within the same functional group, such as annuals, broad-leaved deciduous trees, and broad-leaved evergreen trees, is roughly proportional to S_c (Terashima *et al.*, 2006). Such a positive correlation between g_m and S_c has been found for WT and chloroplast-positioning mutants of Arabidopsis (Tholen *et al.*, 2008). However, there was no correlation between g_{m400} and S_c for the lines used in our present study (Supplementary Fig. S6), possibly due to the fact that the positioning of chloroplasts was normal in the lines that we used and that the range of variation in S_c was not large enough.

Short-term changes in g_m in response to elevated CO_2 are independent of non-structural carbohydrates

Short-term changes in g_m in response to the increase in the CO_2 concentration from 400 ppm to 800 ppm during our photosynthesis measurements were observed in all the carbohydrate-metabolism mutants as well as in the WT (Fig. 3E, F). This suggests that the amount of non-structural carbohydrates was not involved in the short-term changes in g_m. A previous study had shown that g_s and g_m were independently regulated in response to CO_2 concentration during gas-exchange measurements in Arabidopsis WT plants and two mutants of stomatal function, open stomata 1 (*ost1*) and slow-type anion channel 1–2 (*slac1-2*) (Mizokami *et al.*, 2019). Since these plants showed stable g_s and g_m over an hour, the observed changes when the ambient CO_2 concentration was changed from either 400 ppm to 800 ppm or vice versa were not caused by the stress of long-term measurements. In the present study, *pgm1* showed the lowest g_s whereas *cfbp1* showed the lowest g_m. This also suggests that g_s and g_m are not necessarily coordinated well in Arabidopsis. In addition to the short-term changes in g_m, the positive correlations between A_{400} and Rubisco and g_{m400} that we observed were consistent with previous reports (Fig. 4; Flexas *et al.*, 2007b; Tholen *et al.*, 2008; José Javier *et al.*, 2017).

Ecophysiological significance of the down-regulation of photosynthesis

The photosynthetic rate measured at 800 ppm (A_{800}) was significantly lower than that measured at 400 ppm (A_{400}) (Fig. 3A, B), which can be explained by a limitation in triose phosphate use (Sharkey, 1985; Harley and Sharkey, 1991). According to these studies, CO_2 assimilation rate measured at low oxygen concentration reaches a maximum at lower C_i than that measured at normal concentration. In our present study, all the gas-exchange measurements were performed at 1% O_2, which led to a decrease in photosynthetic rate with the increase in C_a and C_i (Woo and Wong, 1983).

The decrease in Rubisco was not observed in *gwd1*, which showed the highest starch content, and in *pgm1*, which showed the highest soluble sugars (Table 1, Fig. 5A, B). This strongly supports the idea that accumulation of soluble sugars and starch does not cause the down-regulation of photosynthesis through the decrease in Rubisco content in Arabidopsis. Although an increase in the content of starch and decreases in Rubisco and A_{400} were found simultaneously only in Col_{LN} (Fig. 5A–D), this would be related to the promotion of leaf senescence and nitrogen remobilization to other organs. Ludewig and Sonnewald (2000) reported that the down-regulation of photosynthesis in tobacco was found in senescing leaves only, and there was no correlation between the transcript levels of photosynthesis-related genes and soluble sugar contents.

It has been argued that the sensitivity of maximum photosynthetic capacity to carbohydrate varies greatly among plant species (Sugiura *et al.*, 2018). Sugiura *et al.* (2015, 2017) showed that *Raphanus sativus*, which in common with Arabidopsis belongs to Brassicaceae, can be classified as a carbohydrate insensitive species. They reciprocally grafted plants with different sink activities and found that neither the maximum photosynthesis nor the Rubisco content was down-regulated even though excessive non-structural carbohydrates were accumulated in the source leaves in shoots grafted to the stock of a variety with a low sink activity. Therefore, it is possible that Brassicaceae can be classified as having carbohydrate-insensitive species. Since carbohydrate-insensitive species such as *R. sativus* and *Glycine max* show increases in CMA in response to accumulation of non-structural carbohydrates, it is possible that the cell wall is also an important carbohydrate sink in the response to changes in the sink–source balance (Sugiura *et al.*, 2017, 2018). Thus, these plants might down-regulated photosynthetic capacity through the suppression of CO_2 conductance by increasing cell wall thickness in order to avoid excess accumulation of non-structural carbohydrates.

Since Rubisco discriminates less against ^{13}C at low concentrations of CO_2 in the chloroplast stroma (C_c), we expected that the $\delta^{13}C$ values of the leaves would reflect C_c, and indeed we found negative correlations between them (Supplementary Fig. S4A, B). Meanwhile, positive correlations were found between $\delta^{13}C$ and starch content for all the lines at both aCO_2 and eCO_2 (Supplementary Fig. S4C, D). Brugnoli *et al.* (1988) found higher $\delta^{13}C$ values in starch than in soluble sugars. They considered that the slower turnover rate of starch is a possible reason, since it would not be available for isotopic exchange for several days, thus resulting in a higher concentration of ^{13}C. Hence, attention should be paid when treating the $\delta^{13}C$ value as an indicator of C_c when non-structural carbohydrates are accumulated excessively.

The Arabidopsis lines that we grew under aCO_2 or eCO_2 showed cell wall thicknesses ranging from 0.195–0.336 μm (Table 1). To confirm our findings, it would be necessary to investigate the relationship between g_m and cell wall thickness in plants over a wider range of wall thickness. It would be possible to obtain plants with thinner cell walls by growing them under low-light conditions (Conn *et al.*, 2011; Lehmeier *et al.*, 2017) and with thicker cell walls by growing them under high-light or more elevated CO_2 conditions (Teng *et al.*, 2006). It would also be interesting to determine the extent to which cell walls become thickened depending on the CO_2 growth conditions. Another issue is to determine interspecific differences in how plastically cell wall thickness and g_m are regulated in the field in response to micro-environmental changes such as temperature (von Caemmerer and Evans, 2015), light intensity, and CO_2 concentration (Tazoe *et al.*, 2009). This would reveal the ecological significance of the down-regulation of photosynthesis.

Conclusions

Our results suggest that elevated CO_2 conditions could decrease mesophyll conductance, g_m, and increase mesophyll resistance, S_c/g_m, through increases in cell wall mass and thickness in Arabidopsis in the long-term. On the other hand, excess starch accumulation had minor effects on g_m and S_c/g_m. We also demonstrated that short-term changes in g_m in response to elevated CO_2 are independent of non-structural carbohydrates in Arabidopsis. Our study provides clues to the ecophysiological

significance of the down-regulation of photosynthesis that are observed under elevated CO_2 conditions.

Supplementary data

Supplementary data are available at *JXB* online.

Fig. S1. Cross-sections of leaves of Arabidopsis grown under 400 ppm or 800 ppm CO_2.

Fig. S2. Electron microscopy of leaves of Arabidopsis grown under 400 ppm or 800 ppm CO_2.

Fig. S3. Relationship between Rubisco content per area and leaf nitrogen content per area in leaves of Arabidopsis grown under 400 ppm or 800 ppm CO_2.

Fig. S4. Relationships between $\delta^{13}C$ and CO_2 concentration in the chloroplast stroma and starch content in leaves of Arabidopsis grown under 400 ppm or 800 ppm CO_2.

Fig. S5. Relationships between cell wall thickness and cell wall mass per area (CMA) and that between CMA and structural leaf mass per area in leaves of Arabidopsis grown under 400 ppm or 800 ppm CO_2.

Fig. S6. Relationship between mesophyll conductance measured at 400 ppm CO_2 and the chloroplast surface area exposed to intercellular space in leaves of Arabidopsis grown under 400 ppm or 800 ppm CO_2.

Acknowledgements

We greatly thank the members of the Laboratory of Plant Ecology in the University of Tokyo and the Laboratory of Crop Science in Nagoya University for their valuable comments and encouragement. This study was supported by Grant-in-Aid for JSPS Research Fellows (nos 25·10531 and 14J07443), and CREST (Creation of essential technologies to utilize carbon dioxide as a resource through the enhancement of plant productivity and the exploitation of plant products).

References

Adachi S, Nakae T, Uchida M, *et al*. 2013. The mesophyll anatomy enhancing CO_2 diffusion is a key trait for improving rice photosynthesis. Journal of Experimental Botany **64**, 1061–1072.

Araya T, Noguchi K, Terashima I. 2006. Effects of carbohydrate accumulation on photosynthesis differ between sink and source leaves of *Phaseolus vulgaris* L. Plant & Cell Physiology **47**, 644–652.

Bernacchi CJ, Morgan PB, Ort DR, Long SP. 2005. The growth of soybean under free air [CO_2] enrichment (FACE) stimulates photosynthesis while decreasing in vivo Rubisco capacity. Planta **220**, 434–446.

Bertin N, Tchamitchian M, Baldet P, Devaux C, Brunel B, Gary C. 1999. Contribution of carbohydrate pools to the variations in leaf mass per area within a tomato plant. New Phytologist **143**, 53–61.

Brugnoli E, Hubick KT, von Caemmerer S, Wong SC, Farquhar GD. 1988. Correlation between the carbon isotope discrimination in leaf starch and sugars of C_3 plants and the ratio of intercellular and atmospheric partial pressures of carbon dioxide. Plant Physiology **88**, 1418–1424.

Cave G, Tolley LC, Strain BR. 1981. Effect of carbon dioxide enrichment on chlorophyll content, starch content and starch grain structure in *Trifolium subterraneum* leaves. Physiologia Plantarum **51**, 171–174.

Cho YH, Yoo SD. 2011. Signaling role of fructose mediated by FINS1/FBP in *Arabidopsis thaliana*. PLoS Genetics **7**, e1001263.

Conn SJ, Gilliham M, Athman A, *et al*. 2011. Cell-specific vacuolar calcium storage mediated by CAX1 regulates apoplastic calcium concentration, gas exchange, and plant productivity in *Arabidopsis*. The Plant Cell **23**, 240–257.

Delucia EH, Sasek TW, Strain BR. 1985. Photosynthetic inhibition after long-term exposure to elevated levels of atmospheric carbon dioxide. Photosynthesis Research **7**, 175–184.

Engelsdorf T, Will C, Hofmann J, *et al*. 2017. Cell wall composition and penetration resistance against the fungal pathogen *Colletotrichum higginsianum* are affected by impaired starch turnover in Arabidopsis mutants. Journal of Experimental Botany **68**, 701–713.

Ethier GJ, Livingston NJ. 2004. On the need to incorporate sensitivity to CO_2 transfer conductance into the Farquhar–von Caemmerer–Berry leaf photosynthesis model. Plant, Cell & Environment **27**, 137–153.

Evans JR, Caemmerer SV, Setchell BA, Hudson GS. 1994. The relationship between CO_2 transfer conductance and leaf anatomy in transgenic tobacco with a reduced content of Rubisco. Functional Plant Biology **21**, 475–495.

Evans JR, Kaldenhoff R, Genty B, Terashima I. 2009. Resistances along the CO_2 diffusion pathway inside leaves. Journal of Experimental Botany **60**, 2235–2248.

Evans JR, Sharkey TD, Berry JA, Farquhar GD. 1986. Carbon isotope discrimination measured concurrently with gas exchange to investigate CO_2 diffusion in leaves of higher plants. Functional Plant Biology **13**, 281–292.

Farquhar GD, Cernusak LA. 2012. Ternary effects on the gas exchange of isotopologues of carbon dioxide. Plant, Cell & Environment **35**, 1221–1231.

Farquhar GD, Sharkey TD. 1982. Stomatal conductance and photosynthesis. Annual Review of Plant Physiology **33**, 317–345.

Flexas J, Diaz-Espejo A, Galmés J, Kaldenhoff R, Medrano H, Ribas-Carbo M. 2007a. Rapid variations of mesophyll conductance in response to changes in CO_2 concentration around leaves. Plant, Cell & Environment **30**, 1284–1298.

Flexas J, Ortuño MF, Ribas-Carbo M, Diaz-Espejo A, Flórez-Sarasa ID, Medrano H. 2007b. Mesophyll conductance to CO_2 in *Arabidopsis thaliana*. New Phytologist **175**, 501–511.

Groszmann M, Osborn HL, Evans JR. 2017. Carbon dioxide and water transport through plant aquaporins. Plant, Cell & Environment **40**, 938–961.

Harley PC, Loreto F, Di Marco G, Sharkey TD. 1992. Theoretical considerations when estimating the mesophyll conductance to CO_2 flux by analysis of the response of photosynthesis to CO_2. Plant Physiology **98**, 1429–1436.

Harley PC, Sharkey TD. 1991. An improved model of C_3 photosynthesis at high CO_2: reversed O_2 sensitivity explained by lack of glycerate reentry into the chloroplast. Photosynthesis Research **27**, 169–178.

Ishikawa-Sakurai J, Hayashi H, Murai-Hatano M. 2014. Nitrogen availability affects hydraulic conductivity of rice roots, possibly through changes in aquaporin gene expression. Plant and Soil **379**, 289–300.

José Javier P-P, Sergio S, Jaume F, Jeroni G. 2017. Cell-level anatomical characteristics explain high mesophyll conductance and photosynthetic capacity in sclerophyllous Mediterranean oaks. New Phytologist **214**, 585–596.

Kitao M, Yazaki K, Kitaoka S, Fukatsu E, Tobita H, Komatsu M, Maruyama Y, Koike T. 2015. Mesophyll conductance in leaves of Japanese white birch (*Betula platyphylla* var. *japonica*) seedlings grown under elevated CO_2 concentration and low N availability. Physiologia Plantarum **155**, 435–445.

Krapp A, Stitt M. 1995. An evaluation of direct and indirect mechanisms for the "sink-regulation" of photosynthesis in spinach: changes in gas exchange, carbohydrates, metabolites, enzyme activities and steady-state transcript levels after cold-girdling source leaves. Planta **195**, 313–323.

Laisk AK. 1977. Kinetics of photosynthesis and photorespiration of C_3 in plants. Moscow: Nauka.

Lanigan GJ, Betson N, Griffiths H, Seibt U. 2008. Carbon isotope fractionation during photorespiration and carboxylation in *Senecio*. Plant Physiology **148**, 2013–2020.

Lehmeier C, Pajor R, Lungren MR, *et al*. 2017. Cell density and airspace patterning in the leaf can be manipulated to increase leaf photosynthetic capacity. The Plant Journal **92**, 981–994.

Ludewig F, Sonnewald U. 2000. High CO_2-mediated down-regulation of photosynthetic gene transcripts is caused by accelerated leaf senescence rather than sugar accumulation. FEBS Letters **479**, 19–24.

Mizokami Y, Noguchi K, Kojima M, Sakakibara H, Terashima I. 2015. Mesophyll conductance decreases in the wild type but not in an

ABA-deficient mutant (*aba1*) of *Nicotiana plumbaginifolia* under drought conditions. Plant, Cell & Environment **38**, 388–398.

Mizokami Y, Noguchi K, Kojima M, Sakakibara H, Terashima I. 2019. Effects of instantaneous and growth CO_2 levels, and ABA on stomatal and mesophyll conductances. Plant, Cell &, Environment **42**, 1257–1269.

Mori IC, Rhee J, Shibasaka M, Sasano S, Kaneko T, Horie T, Katsuhara M. 2014. CO_2 transport by PIP2 aquaporins of barley. Plant & Cell Physiology **55**, 251–257.

Nafziger ED, Koller HR. 1976. Influence of leaf starch concentration on CO_2 assimilation in soybean. Plant Physiology **57**, 560–563.

Nakano H, Muramatsu S, Makino A, Mae T. 2000. Relationship between the suppression of photosynthesis and starch accumulation in the pod-removed bean. Functional Plant Biology **27**, 167–173.

Periappuram C, Steinhauer L, Barton DL, Taylor DC, Chatson B, Zou J. 2000. The plastidic phosphoglucomutase from *Arabidopsis*. A reversible enzyme reaction with an important role in metabolic control. Plant Physiology **122**, 1193–1199.

Poorter H, Pepin S, Rijkers T, de Jong Y, Evans JR, Körner C. 2006. Construction costs, chemical composition and payback time of high- and low-irradiance leaves. Journal of Experimental Botany **57**, 355–371.

Pritchard SG, Peterson CM, Prior SA, Rogers HH. 1997. Elevated atmospheric CO_2 differentially affects needle chloroplast ultrastructure and phloem anatomy in *Pinus palustris*: interactions with soil resource availability. Plant, Cell & Environment **20**, 461–471.

Sawada S, Kuninaka M, Watanabe K, Sato A, Kawamura H, Komine K, Sakamoto T, Kasai M. 2001. The mechanism to suppress photosynthesis through end-product inhibition in single-rooted soybean leaves during acclimation to CO_2 enrichment. Plant & Cell Physiology **42**, 1093–1102.

Scafaro AP, Von Caemmerer S, Evans JR, Atwell BJ. 2011. Temperature response of mesophyll conductance in cultivated and wild *Oryza* species with contrasting mesophyll cell wall thickness. Plant, Cell & Environment **34**, 1999–2008.

Schneider CA, Rasband WS, Eliceiri KW. 2012. NIH Image to ImageJ: 25 years of image analysis. Nature Methods **9**, 671–675.

Sheen J. 1994. Feedback control of gene expression. Photosynthesis Research **39**, 427–438.

Sharkey TD. 1985. Photosynthesis in intact leaves of C_3 plants: physics, physiology and rate limitations. The Botanical Review **51**, 53–105.

Sugiura D, Betsuyaku E, Terashima I. 2015. Manipulation of the hypocotyl sink activity by reciprocal grafting of two *Raphanus sativus* varieties: its effects on morphological and physiological traits of source leaves and whole-plant growth. Plant Cell & Environment **38**, 2629–2640.

Sugiura D, Betsuyaku E, Terashima I. 2018. Interspecific differences in how sink–source imbalance causes photosynthetic downregulation among three legume species. Annals of Botany **123**, 715–726.

Sugiura D, Watanabe CKA, Betsuyaku E, Terashima I. 2017. Sink–source balance and down-regulation of photosynthesis in *Raphanus sativus*: effects of grafting, N and CO_2. Plant & Cell Physiology **58**, 2043–2056.

Tazoe Y, von Caemmerer S, Badger MR, Evans JR. 2009. Light and CO_2 do not affect the mesophyll conductance to CO_2 diffusion in wheat leaves. Journal of Experimental Botany **60**, 2291–2301.

Tazoe Y, von Caemmerer S, Estavillo GM, Evans JR. 2011. Using tunable diode laser spectroscopy to measure carbon isotope discrimination and mesophyll conductance to CO_2 diffusion dynamically at different CO_2 concentrations. Plant, Cell & Environment **34**, 580–591.

Teng N, Wang J, Chen T, Wu X, Wang Y, Lin J. 2006. Elevated CO_2 induces physiological, biochemical and structural changes in leaves of *Arabidopsis thaliana*. New Phytologist **172**, 92–103.

Terashima I, Hanba YT, Tazoe Y, Vyas P, Yano S. 2006. Irradiance and phenotype: comparative eco-development of sun and shade leaves in relation to photosynthetic CO_2 diffusion. Journal of Experimental Botany **57**, 343–354.

Terashima I, Hanba YT, Tholen D, Niinemets Ü. 2011. Leaf functional anatomy in relation to photosynthesis. Plant Physiology **155**, 108–116.

Thain JF. 1983. Curvature correction factors in the measurement of cell surface areas in plant tissues. Journal of Experimental Botany **34**, 87–94.

Tholen D, Boom C, Noguchi K, Ueda S, Katase T, Terashima I. 2008. The chloroplast avoidance response decreases internal conductance to CO_2 diffusion in *Arabidopsis thaliana* leaves. Plant, Cell & Environment **31**, 1688–1700.

von Caemmerer S, Evans JR. 2015. Temperature responses of mesophyll conductance differ greatly between species. Plant, Cell & Environment **38**, 629–637.

Walker BJ, Cousins AB. 2013. Influence of temperature on measurements of the CO_2 compensation point: differences between the Laisk and O_2-exchange methods. Journal of Experimental Botany **64**, 1893–1905.

Wingate L, Seibt U, Moncrieff JB, Jarvis PG, Lloyd J. 2007. Variations in ^{13}C discrimination during CO_2 exchange by *Picea sitchensis* branches in the field. Plant, Cell & Environment **30**, 600–616.

Woo KC, Wong SC. 1983. Inhibition of CO_2 assimilation by supraoptimal CO_2: effect of light and temperature. Functional Plant Biology **10**, 75–85.

Zeeman SC, Smith SM, Smith AM. 2004. The breakdown of starch in leaves. New Phytologist **163**, 247–261.

Zhu C, Ziska L, Zhu J, Zeng Q, Xie Z, Tang H, Jia X, Hasegawa T. 2012. The temporal and species dynamics of photosynthetic acclimation in flag leaves of rice (*Oryza sativa*) and wheat (*Triticum aestivum*) under elevated carbon dioxide. Physiologia Plantarum **145**, 395–405.